ANALYSIS OF FREQUENCY RESPONSES OF MODEL FLOWS OF LIQUID IN TRICKLE BEDS

Vladimír Staněk and Milan Čársky

Institute of Chemical Process Fundamentals, Czechoslovak Academy of Sciences, 165 02 Prague 6 - Suchdol

Received November 20th, 1981

Frequency responses have been derived for four mathematical models of the trickle flow in a packed bed column. The models contain gradually one to four parameters. Asymptotic expressions have been also obtained for the frequency responses under large values of the Peclet number. A possibility has been tested of using the complex arithmetic feature of a computer to evaluate numerically the model responses and to separate the real and the imaginary part of the response. Analysis has shown that all four models can be discriminated and their parameters are observable in the complex plane. This approach thus appears plausible for processing real experimental data as well as for the discrimination between various models.

The counter-current arrangement of the flow of liquid and gas has been currently utilized in a number of processes involving the transfer of mass and heat (absorption, absorption with chemical reaction, distillation, catalytic operations, *etc.*) as it provides for intensive contact of the phases and large driving forces for interfacial transport. The liquid phase is uniformly spread over the column cross section by means of a suitable distributor of liquid and trickles down in the form of rivulets or film: the gas streams in the opposite direction. Under suitable conditions a considerably large interfacial surface is created.

There are two limiting idealized flow situations for the flow of a fluid: "the plug flow" and the "ideal mixer". Real flows in continuously operated equipment fall between these two extremes. Groenhof[1] reports that the liquid need not flow in the form of a film over the surface of the packing but may form droplets or rivulets. Chanelling may also occur when part of the liquid follows faster preferential paths than the rest of the liquid on the packing. This phenomenon is due to the inhomogeneous structure of the bed together with the action of the gravity forces and surface tension. The preferential channels do not change appreciably with time. In small diameter columns with respect to the particle diameter, much of the liquid often flows down the column wall. Groenhof[2] reports that this phenomenon, the so called "wall effect" becomes manifest in columns where

$$d_c/d_p < 10 . \qquad (1)$$

Other works[1,3], however, recommend even greater values of this ratio, especially for the packing of Raschig rings if the wall flow is to be negligible.

Another manifestation of the real flow in a packed bed column is the existence of the zones with nearly stagnant liquid. This liquid clings to the packing predominantly at the points of contact between individual elements of the packing, between the elements of the packing and the column wall or in region with very low local flow rate. The specific volume of the column occupied by the stagnant liquid under a given flow rate of the liquid phase then determines the stagnant liquid hold-up. Between the stagnant and the dynamic region then may occur the exchange of mass, but the mechanism of this exchange has not been specified to date. All the described manifestations of the real flow of phases in a trickle bed column diminish the effective interfacial surface for mass transfer and thus affect mostly adversely the operation of the separation equipment. Changes of conversion and selectivity occur in chemical reactors. Patwardhan[3,4], for instance, defined an effective interfacial surface for absorption accompanied by chemical reaction as follows

$$a_{ef} = a_d + f a_s . \qquad (2)$$

The coefficient f was defined as a ratio of the rate of absorption into the stagnant and the dynamic region. For a second order reaction Patwardhan expresses f as a function of diffusivity, the enhancement factor, concentration, the coefficient of interfacial transfer and the rate of exchange of mass between the stagnant and the dynamic region.

The real states of the flow of liquid between the limiting situations, but closer to the plug flow, may be described by the mechanism of axial and radial dispersion. Axial dispersion is mostly an undesirable phenomenon, diminishing local concentration driving forces for interfacial transfer and hence the efficiency of separation equipment or conversion in chemical reactors[5-7]. On the contrary radial dispersion, which in design calculations has been often neglected, plays frequently a positive role by diminishing radial temperature gradients. However, attempts to increase radial dispersion (*e.g.* by increased size of particles) may be accompanied by increased axial dispersion[7]. The degree of mixing in a bed of packing depends on the mechanism of the flow, molecular diffusitivites of individual components and the geometry of the packing in a manner that has not been so far fully elucidated.

The above described phenomena in combination form the characteristic picture of the real flow of liquid departing from the idealized forms of the mathematical descriptions. At the same time it is apparent that physically best founded would be the description (model) which accounts for each nonideality by an individualized, not lumped, parameter. Nevertheless, practical design calculations of trickle bed equipment utilize mostly the plug flow or the axially dispersed plug flow model.

An important parameter of the various models and a characteristic of the hydrodynamics of the flow is the hold-up of liquid in its different forms dependent on the measuring method and definition in the corresponding model representation. The hold-up of liquid in a trickle bed column affects on the one hand the extent of the area of cross section available for the flow of gas and hence also the pressure drop under the two phase flow. Further also the turbulence, which together with the increased wetted surface intensifies the interfacial transport. In apparatuses with chemical reactions especially the slow reactions, the hold-up of liquid affects the yield and selectivity, in dependence on the extent to which the conversion takes place within the interfacial film and the bulk of liquid. The magnitude of the liquid hold-up is affected by the flow rates of phases, their physical properties and the geometry of the packed layer.

Currently used experimental method for the determination of the dynamic hold-up of liquid consists of sudden disconnection of the feeds of the gas and the liquid phases and collection of the draining liquid[5,6,10-12]. Static hold-up then follows from the difference of the volume of liquid charged into the dry column and the volume of the drained liquid[5,11]. At this point

it is necessary to note the difference between the stagnant hold-up (h_s) and the static hold-up (h_{si}). The static hold-up is formed by the liquid held in the bed by the action of the surface forces even after a long period after the shut off of the flows of phases. On the other hand, the stagnant hold-up is formed by the liquid occupying the stagnant regions in the bed at non-zero flow rate of liquid[4,8]. The results of some authors[13,14], however, show that the static hold-up understood as given above loses entirely its physical meaning under the flowing conditions.

Bennett and Goodridge[9] considered in their work the axially dispersed flow of liquid in the dynamic region and a slow exchange of mass with the stagnant region characterized by a coefficient of mass exchange. The value of this coefficient was independent of the flow rate of gas while rapidly increased with increasing flow rate of liquid. The authors presumed independence of the mentioned coefficient on the size of the packing element and further found that the ratio of the stagnant to the dynamic hold-up is independent of the flow rate of gas and decreases with the flow rate of liquid. The coefficient of axial dispersion is another important parameter. It must be born in mind, however, that numerical values of dispersivity depend fundamentally on the formulation of the model applied to process experimental data. Linek and coworkers[5] found greater values of the coefficient of axial dispersion in the liquid phase than in the gas. Axially dispersed character of the liquid phase flow was considerably affected by the magnitude of the mass transfer coefficient. The difference between values of the mass transfer coefficient computed from the plug flow model and the axially dispersed model reached as much as 50% of the value of the coefficient based on the plug flow.

Dunn and coworkers[6] report that axial dispersion in the liquid phase is independent of the gas phase flow rate, decreases with the increasing velocity of liquid and is substantially greater than the axial dispersion in the gas phase.

The aim of this work has been to derive the transfer functions for a series of model flows of the liquid phase under the conditions of the two-phase counter-current flow, their transformation into the frequency domain and the examination of observability of the model parameters from experimental frequency responses. The examined models are formulated in the form of differential equations easily amenable for modelling the flow interactions with the interfacial transport of mass, heat and the course of chemical reactions.

THEORETICAL

Starting from a balance of dissolved species over an infinitesimal section of the column length the following equation is obtained for the case of the plug flow (PF), assuming equal velocity of the flow at all points of the bed

$$v\,\partial c/\partial z + h\,\partial c/\partial t = 0\,, \tag{3}$$

where h designates the total hold-up of liquid.

Upon admitting the existence of the stagnant zones, (model SZ), characterized by the stagnant liquid hold-up, h_s, while in the dynamic part, of the extent given by the dynamic liquid hold-up, h_d, the liquid flows in plug flow, the balance of the

dissolved species is given by

$$q(c - c_s) + v\,\partial c/\partial z = -h_d\,\partial c/\partial t\,, \tag{4}$$

where c_s designates concentration in the stagnant liquid. The coefficient q quantifies the intensity of mass exchange between the stagnant and the dynamic part of the liquid hold-up while the balance of the dissolved species in the stagnant liquid takes the following form

$$q(c - c_s) = h_s\,\partial c_s/\partial t\,. \tag{5}$$

The axially dispersed model (AD) superimposes axial dispersion on the plug flow of liquid. The corresponding balance of dissolved species thus takes the following form where D designates the coefficient of axial dispersion

$$v\,\partial c/\partial z - Dh\,\partial^2 c/\partial z^2 = -h\,\partial c/\partial t\,. \tag{6}$$

Upon assuming at the same time also the existence of the stagnant zones, together with the axial dispersion, the balance of the dissolved species in the dynamic liquid is as follows:

$$v\,\partial c/\partial z - Dh_d\,\partial^2 c/\partial z^2 + q(c - c_s) = -h_d\,\partial c/\partial t\,. \tag{7}$$

The balance in the stagnant liquid remains identical with Eq. (5). This, from the view point of the number of parameters the most complex model (ADSZ), is formally identical with the model proposed by Bennett and Goodridge[9]. By separation of the axial dispersion from the effect of the stagnant zones one must expect also a fundamentally different numerical values of, for instance, the dispersion coefficient, D.

Let us now define a quantity $C = c - c_{stac}$, where c_{stac} is the steady state composition of liquid, introduce this quantity into Eqs (3)–(7) and perform the Laplace transform. For the case of the PF model one obtains

$$v\,\mathrm{d}\bar{C}/\mathrm{d}z + hs\bar{C} = 0 \tag{8}$$

which for the boundary condition

$$\bar{C} = \bar{C}_0 \quad \text{for} \quad z = 0 \tag{9}$$

yields

$$\bar{C} = \bar{C}_0 \exp(-hsz/v)\,. \tag{10}$$

The transfer function for the response of the composition of the outlet liquid to a concentration change in the inlet liquid may be written in the form

$$G(s) = \bar{C}_Z/\bar{C}_0 = \exp(-\tau s)\,, \tag{11}$$

where $\tau = hZ/v$ is the residence time of liquid in the system. In a similar fashion one can proceed also in the derivation of the transfer functions for the SZ, AD and the ADSZ models.

In the case of the SZ model one obtains from Eqs (*4*) and (*5*) a single first-order differential equation to be solved with the boundary condition (*9*). The transfer function then may be written in the form

$$G(s) = \bar{C}_Z/\bar{C}_0 = \exp(-AZ), \tag{12}$$

where

$$A = \frac{1}{v}\left(q - \frac{q^2}{h_s s + q} + h_d s\right). \tag{13}$$

In the case of the AD model we obtain the following equation

$$(Z/Pe)(d^2\bar{C}/dz^2) - (d\bar{C}/dz) - (\tau s/Z)\,\bar{C} = 0. \tag{14}$$

Appropriate boundary conditions for this system are the conditions formulated by Danckwerts[15]

$$\bar{C}_0 = (\bar{C})_{z=0+} - (Z/Pe)(d\bar{C}/dz)_{z=0+} \quad \text{for} \quad z = 0 \tag{15}$$

$$d\bar{C}/dz = 0 \quad \text{for} \quad z = Z. \tag{16}$$

For the transfer function then follows

$$G(s) = \frac{4\sqrt{(1 + 4\tau s/Pe)}}{[1 + \sqrt{(1 + 4\tau s/Pe)}]^2 \exp(-\lambda_2 Z) - [1 - \sqrt{(1 + 4\tau s/Pe)}]^2 \exp(-\lambda_1 Z)} \tag{17}$$

where

$$Z\lambda_{1,2} = (Pe/2)[1 \pm \sqrt{(1 + 4\tau s/Pe)}]. \tag{18}$$

For the case of the ADSZ model one obtains from Eqs (*5*) and (*7*) a single second-order differential equation:

$$\frac{Z}{Pe_d}\frac{d^2\bar{C}}{dz^2} - \frac{d\bar{C}}{dz} - \left(\frac{\tau_d s}{Z} + \frac{q h_s s}{v(q + h_s s)}\right)\bar{C} = 0. \tag{19}$$

Upon using the boundary conditions (*15*) and (*16*) with the *Pe* number replaced

by Pe_d, the following form of the transfer function results

$$G(s) = \frac{4B}{(1 + B)^2 \exp(-\lambda_4 Z) - (1 - B)^2 \exp(-\lambda_3 Z)}, \tag{20}$$

where

$$B = \sqrt{\left[1 + \frac{4Z}{Pe_d}\left(\frac{\tau_d s}{Z} + \frac{q h_s s}{v(q + h_s s)}\right)\right]}$$

and

$$Z\lambda_{3,4} = \frac{Pe_d}{2}\left\{1 \pm \sqrt{\left[1 + \frac{4}{Pe_d}\left(\tau_d s + \frac{Z q h_s s}{v(q + h_s s)}\right)\right]}\right\}. \tag{21}$$

Formally one derives for the SZ and the ADSZ models also the transfer functions for the concentration in the stagnant liquid. This quantity, however, is not measurable and the corresponding transfer function therefore has no practical significance.

Substituting $s = i\omega$, the original Laplace transform changes to the Fourier transform. From the transfer functions one thus obtains complex variable functional relationships, or the frequency responses to a harmonic perturbation with the frequency as a variable

$$G(i\omega) = \exp(-\tau i\omega) \tag{11a}$$

for the PF model

$$G(i\omega) = \exp\left[-(E_1 + iF_1) Z\right] \tag{12a}$$

for the *SZ* model where

$$E_1 = \frac{1}{v}\left(q - \frac{q^3}{q^2 + h_s^2\omega^2}\right), \quad F_1 = \frac{1}{v}\left(h_d\omega + \frac{q^2 h_s \omega}{q^2 + h_s^2\omega^2}\right). \tag{13a}$$

In the transformation of the transfer functions into the frequency domain for the models incorporating axial dispersion, *i.e.* the AD and the ADSZ models, we shall effect an additional simplification based on the finding that for current values of axial dispersivity and not excessively short column, one of the pair of the characteristic values $(Z\lambda_{1,2})$ and $(Z\lambda_{3,4})$, given by Eqs (*18*) and (*21*) is always a large positive number. With a sufficient accuracy one may put then the expressions $\exp(-\lambda_1 Z)$ and $\exp(-\lambda_3 Z)$ equal to zero.

With this simplification we obtain

$$G(i\omega) = \frac{4\sqrt{(1 + 4\tau i\omega/Pe)}}{\left[1 + \sqrt{(1 + 4\tau i\omega/Pe)}\right]^2} \exp(\lambda_2 Z) \tag{17a}$$

for the AD model and

$$G(i\omega) = 4B \exp(\lambda_4 Z)/(1 + B)^2 \qquad (20a)$$

for the ADSZ model, where

$$B = \sqrt{\left[1 + \frac{4Z}{Pe_d}\left(\frac{\tau_d i\omega}{Z} + \frac{qh_s i\omega}{v(q + h_s i\omega)}\right)\right]}.$$

The justification of the simplification leading to the above expression, *i.e.* of the assumption that $4\tau\omega/Pe \ll 1$ may be tested with the aid of the following approximate expressions valid for the given conditions

$$Z\lambda_1 \approx Pe + \tau i\omega \approx Pe \qquad (22)$$

$$Z\lambda_2 \approx -\tau i\omega \qquad (23)$$

for the AD model and, similarly for the ADSZ model, we shall obtain the following approximations

$$Z\lambda_3 \approx Pe_d\,, \quad Z\lambda_4 \approx -i\omega[\tau_d + Zqh_s/(v(q + h_s i\omega))]\,. \qquad (24)$$

Making use of the large value of the Peclet number with the depth of the packed section as a characteristic parameter (sometimes also the Bode number) to effect simplifications one step further, the expressions in Eqs (*17a*) and (*20a*) change to

$$G(i\omega) = \exp(\lambda_2 Z) \qquad (17b)$$

for the AD model and

$$G(i\omega) = \exp(\lambda_4 Z) \qquad (20b)$$

for the ADSZ model.

These simplified forms of the frequency responses are particularly advantageous for the optimization of the model parameters. Owing to the inherent nonlinearity of the models with respect to the parameters one must use numerical routines of optimizations calling for repeated calculations of the frequency responses and, eventually, their derivatives with respect to the parameters. The simplified expressions for the frequency responses thus considerably contribute to the time efficiency of the developed algorithms. In addition, if the employed simplification proves to be insufficiently accurate, the localization of the optimum may be improved by a few extra iterations while employing the more accurate expression for the frequency response.

The ADSZ models incorporates implicitly all three previous simpler models. For instance, in the limit $D \to 0$ the ADSZ model reduces to the SZ model; to the AD model reduces in the limits $q \to \infty$ (the hold-up represented by the sum $h_d + h_s$) or in the limit $h_s \to 0$ (the hold-up represented by h_d). A combination of the limit $D \to 0$ with some of the other limits reduces the ADSZ model down to the PF model. Analogously to the PF model reduce the SZ model (in the limit $h_s \to 0$ and hence also for $h_d \to h$) and the AD model (in the limit $D \to 0$).

The frequency response of the system may be generally expressed in the form

$$G(i\omega) = R \exp(i\varphi), \tag{25}$$

where R is the amplitude ratio of the outlet to the input signal and φ is the phase shift (lag) of the outlet signal with respect to the input. A comparison of Eq. (25) with the expressions for the frequency responses of the PF and the SZ models (Eqs (11a), (12a)) shows clearly that in these cases we can find direct explicit expressions for R and φ. In case of the AD and the ADSZ models (Eqs (17a), (20a)) the real and the imaginary part of the frequency responses cannot be separated analytically, R and φ thus cannot be expressed explicitly.

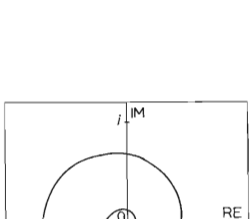

FIG. 1

Frequency response $G(i\omega)$ computed for the axially dispersed model $v = 7{\cdot}64 \,.\, 10^{-3}$ m/s, $h = 0{\cdot}1258$, $D = 2{\cdot}308 \,.\, 10^{-3}$ m^2/s. Abscissa: real part of $G(i\omega)$, ordinate: imaginary part of $G(i\omega)$

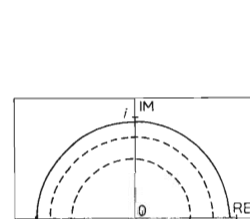

FIG. 2

Part of frequency response $G(i\omega)$ computed for the axially dispersed model $v = 7{\cdot}864 \,.\, 10^{-3}$ m/s, $h = 0{\cdot}1258$, $D = 2{\cdot}308 \,.\, 10^{-4}$ m^2/s in the frequency range $\omega = 0-0{\cdot}63$ rad/s

CALCULATIONS

The calculations of the frequency responses were performed on an EC-1033 computer using its complex arithmetics feature enabling numerical separations of the real and the imaginary part for given values of the parameters and frequency of the input signal. For the AD and the ADSZ models the calculations were carried out using Eqs (*17a*) and (*20a*). In the opposite case, *i.e.* using expressions with both characteristic values λ, numerical difficulties were experienced stemming from the fact that the value $\lambda_1 Z$ (or $\lambda_3 Z$) fluctuated around the limit causing the underflow in the exponent. These difficulties, although not fatal for the evaluation of the responses proper, may bring about total failure of the routine performing numerical evaluation of the derivatives with respect to the parameters, necessitated in the optimization routine employed.

The computed frequency responses shall be shown graphically in the form of the Nyqyist's diagrams. These diagrams plot on the horizontal axis the real part of the response, while the imaginary part is on the vertical axis, with the frequency as a parameter. Fig. 1 shows a typical response of the AD model.

The frequency response derived from the PF model takes in the complex plane always the form of a circle of unit radius independently of the flow rate (for non-zero h). This is so because the plug flow does not predict any amplitude damping of the

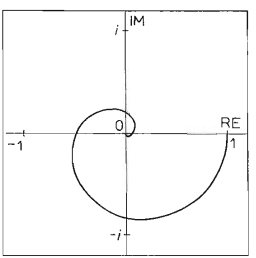

FIG. 3

Frequency response $G(i\omega)$ computed for the axially dispersed model $v = 7{\cdot}864 \cdot 10^{-3}$ m/s, $h = 0{\cdot}1258$, $D = 2{\cdot}308 \cdot 10^{-2}$ m^2/s

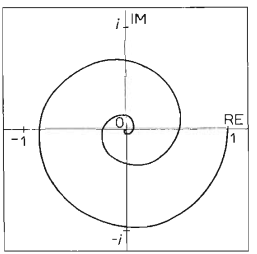

FIG. 4

Frequency response $G(i\omega)$ computed for the model with stagnant zones $v = 7{\cdot}864 \cdot 10^{-3}$ m/s, $h_d = 6{\cdot}85 \cdot 10^{-2}$, $q = 4{\cdot}617 \cdot 10^{-2}$ s^{-1}, $h_s = 5{\cdot}76 \cdot 10^{-2}$

input concentration signal but merely its shift. As already mentioned the limit $D \to 0$ reduces the AD model to the PF model. Fig. 2 shows the frequency response of the same model as in Fig. 1 with a tenfold decrease of the coefficient D. On the contrary in the limit $D \to \infty$ the model approaches the ideal mixer. Fig. 3 shows the function $G(i\omega)$ for the AD model as in Fig. 1 but with a tenfold increase of the coefficient D. Fig. 4 shows the frequency response derived from the SZ model in the complex plane. In the limit $h_s \to 0$ (and hence $h_d \to h$) the SZ model reduces to PF model. Fig. 5 shows part of the frequency response as that in Fig. 4 for the case $h_s = 0{\cdot}1\ h_d$. Fig. 6 shows the frequency response for the most sophisticated model examined in this work, the ADSZ model.

CONCLUSIONS

Analysis of the derived transfer functions has shown that the parameters of the four examined models are observable and that the models can be discriminated from the frequency responses in the form of the Nyqyist's diagrams.

The frequency responses of the models incorporating axial dispersion may be conveniently studied with the aid of the complex arithmetics of a computer employed to separate numerically the real and the imaginary part. The analysis may be facilitated when using the asymptotic forms of the expressions for the frequency responses.

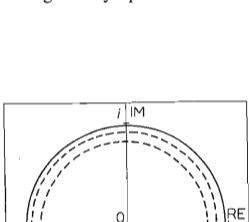

FIG. 5

Part of frequency response $G(i\omega)$ for the model with stagnant zones $v = 7{\cdot}864 \cdot 10^{-3}$ m/s, $h_d = 0{\cdot}1146$, $q = 4{\cdot}617 \cdot 10^{-2}\ s^{-1}$, $h_s = 1{\cdot}146 \cdot 10^{-2}$ in the frequency range $\omega = 0$—$0{\cdot}63$ rad/s

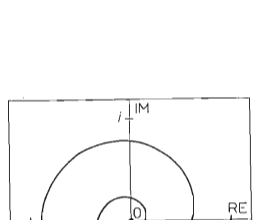

FIG. 6

Frequency response $G(i\omega)$ for the axially dispersed model with stagnant zones $v = 7{\cdot}864 \cdot 10^{-3}$ m/s, $h_d = 7{\cdot}1 \cdot 10^{-2}$, $h_s = 6{\cdot}1 \cdot 10^{-2}$, $q = 5{\cdot}95 \cdot 10^{-2}\ s^{-1}$, $D = 1 \cdot 10^{-4}\ m^2/s$

The study of the frequency responses in the complex plane appears particularly attractive in those cases when an explicit expression for the phase shift cannot be found. In this case numerical methods transform the shift into the interval $0-2\pi$, which, of course, poses no problem for plotting in the phase plane. On the contrary, processing into the form of the Bode diagrams (amplitude ratio and phase lag as functions of the frequency) requires total phase shift, including its integer multiples of the full angle.

The proposed form of discriminating between models in the complex plane standardizes the routine of parameter evaluation and removes the bias encompassed in the parameter evaluation based separately on the amplitude ratio and the phase lag.

LIST OF SYMBOLS

a	specific interfacial surface [m^2/m^3]
A	defined in Eq. (*13*)
B	defined in Eq. (*20*)
c	concentration [k mol/m^3]
$C = c - c_{\text{stac}}$	concentration [k mol/m^3]
d	diameter [m]
D	coefficient of axial dispersion [m^2/s]
E_1, F_1	defined in Eq. (*13a*)
f	coefficient in Eq. (*2*)
$G(i\omega)$	frequency response
$G(s)$	transfer function
h	specific hold-up of liquid [m^3/m^3]
Im	imaginary part of a complex number
$Pe = vZ/Dh$	Peclet number
$Pe_d = vZ/Dh_d$	Peclet number
q	coefficient of mass exchange between the dynamic and stagnant liquid [s^{-1}]
R	amplitude ratio
R^E	real part of a complex number
s	Laplacian variable [s^{-1}]
t	time [s]
v	superfacial velocity of liquid [m/s]
z	axial coordinate
Z	depth of packed layer [m]
$\lambda_{1,2}$	defined in Eq. (*18*)
$\lambda_{3,4}$	defined in Eq. (*21*)
ω	circular frequency [rad/s]
$\tau = hZ/v$	mean residence time [s]
$\tau_d = h_dZ/v$	mean residence time [s]
φ	phase lag [rad]

Subscripts

s	stagnant liquid
0	inlet end ($z = 0$)

Z outlet end ($z = Z$)
c column
st static
stac steady state
ef effective
d dynamic liquid
p packing

REFERENCES

1. Groenhof H. C.: Chem. Eng. J. *14*, 193 (1977).
2. Groenhof H. C.: Chem. Eng. J. *14*, 181 (1977).
3. Patwardhan V. S.: Can. J. Chem. Eng. *56*, 558 (1978).
4. Patwardhan V. S.: Can. J. Chem. Eng. *56*, 56 (1978).
5. Linek V., Beneš P., Sinkule J., Křivský Z.: Ind. Eng. Chem. Fundam. *17*, 298 (1978).
6. Dunn W. E., Vermeulen T., Wilke C. R., Word T. T.: Ind. Eng. Chem. Fundam. *16*, 116 (1977).
7. Gunn D. J., Pryce C.: Trans. Inst. Chem. Eng. *47*, T341 (1969).
8. Villermaux J., Van Swaaij W. P. M.: Chem. Eng. Sci. *24*, 1097 (1969).
9. Bennett A., Goodridge F.: Trans. Inst. Chem. Eng. *48*, T232 (1970).
10. Varrier C. B. S., Rao K. R.: Trans. Ind. Inst. Chem. Eng. *13*, 29 (1960–61).
11. Furnas C. C., Bellinger F.: Trans. Amer. Inst. Chem. Eng. *34*, 251 (1938).
12. Elgin J. C., Weiss F. B.: Ind. Eng. Chem. *31*, 435 (1939).
13. Staněk V., Kolář V.: This Journal *38*, 1012 (1973).
14. Staněk V., Kolář V.: Chem. Eng. J. *5*, 51 (1973).
15. Danckwerts P. V.: Chem. Eng. Sci. *2*, 1 (1953).

Translated by author (V. S.).